Plankton Benthos Res 16(3): 191–199, 2021

Plankton & Benthos Research

Aquatic invertebrate's Carbohydrate-binding module assists environmental cellulase to immobilize in wetland sediments

Wen Liu[1,*], Hiroshi Kamitakahara[2], Shingo Maegawa[3] & Haruhiko Toyohara[4]

[1] *Graduate School of Global Environmental Studies, Kyoto University, Kyoto 606–8317, Japan*
[2] *Division of Forest and Biomaterials Science, Graduate School of Agriculture, Kyoto University, Kyoto 606–8502, Japan*
[3] *Department of Intelligence Science and Technology, Graduate School of Informatics, Kyoto University, Kyoto, 606–8507 Japan*
[4] *Faculty of Agriculture, Setsunan University, Osaka 573–0101, Japan*

Received 22 October 2020; Accepted 11 January 2021 Responsible Editor: Gen Kanaya

doi: 10.3800/pbr.16.191

Abstract: Carbohydrate-binding modules (CBMs) are non-catalytic protein domains that bind to carbohydrates, and have been well studied in microorganisms. Endogenous CBMs in aquatic invertebrates, however, have not yet been identified, and little is known about their ecological significance to wetland environments. Using an approach of characterizing a recombinant CBM (*Cj*Cel9A) from a brackish bivalve, *Corbicula japonica*, this work identified *Cj*Cel9A-CBM's cellulose-binding activity. Scatchard plot analysis in the study of *Cj*Cel9A-CBM binding to *α*-cellulose showed a high corresponding partitioning coefficient (K_r) of 20.33, indicating *Cj*Cel9A-CBM's high affinity for cellulose. In addition, this affinity tolerated a high ion concentration buffer system, consistent with *C. japonica*'s adaption to brackish wetland environments. Moreover, immuno-scanning electron microscopy (immuno-SEM) suggested that *Cj*Cel9A-CBM binds to *α*-cellulose unevenly, which was further determined to be caused by its higher affinity for crystalline cellulose (Cellulose I, mostly seen in plant leaves). Together, these findings suggest that *Cj*Cel9A-CBM is capable of immobilizing its associated catalytic domain on environmental crystalline cellulose (i.e., fallen leaves) in wetland sediments. Most importantly, they could provide a reasonable answer to a question recognized broadly in wetland ecologists, namely, why many wetland sediments have constant cellulase activities, although the sediments are being washed almost every day.

Key words: Aquatic invertebrate, Carbohydrate-binding modules (CBMs), cellulose decomposition, wetland

Introduction

During the study of the mechanism by which filter-feeding bivalves consume cellulose, our previous findings revealed that a Japanese endemic bivalve, namely *Corbicula japonica*, secretes its endogenous cellulase (*Cj*Cel9A) into wetland sediments (Liu et al. 2019). Also, immunological methods detected the existence of *Cj*Cel9A cellulase in the sediment of *C. japonica*'s habitat, indicating that *Cj*Cel9A could somehow be immobilizing itself in wetland sediment, preventing it from being washed away. However, the mechanism remains unknown.

By investigating the structure of *Cj*Cel9A, we showed that *Cj*Cel9A has a Family 2 CBM linked to the 5′ side of the catalytic domain (Sakamoto et al. 2007, Carbohydrate-Active enZYmes Database; CAZY Database). Carbohydrate-binding modules were first reported in fungus (Tilbeurgh et al. 1986, Tomme et al. 1988), when their cellulolytic system was studied. CBMs are non-catalytic protein domains present in glycoside hydrolases. CBMs bind to carbohydrates, including those in plant cell-wall structures. CBMs of bacterial and fungal origin have been studied for decades regarding their substrate specificities and affinity levels (Boraston et al. 2004, Shosevov et al. 2006). In contrast, there have been no studies focused on the molecular functions of aquatic invertebrates' CBMs. Examination of the database of CBMs (Carbohydrate-Active enZYmes Database) shows that most aquatic invertebrates' CBMs are putative ones, identified only by

* Corresponding author: Wen Liu; E-mail, 7s@kyoto-u.ac.jp

their nucleotide/amino acid sequences. Many invertebrate CBMs in the database were found as a "by-product" of studies of their partner glycoside hydrolases (Suzuki et al. 2003, Li et al. 2009, Sakamoto et al. 2009). In some cases, CBMs of aquatic invertebrates have also been revealed by total cDNA cloning or genome studies for other research purposes (National Center for Biotechnology Information (Genbank). The lack of much detailed information might be ascribed to the late discovery of the existence of endogenous cellulases and CBMs in invertebrates (Watanabe & Tokuda 2001). Tanimura et al. (2013) summarized the aquatic invertebrates that possess endogenous cellulases. Among them, multi-domain cellulases with CBMs were also found, but those CBMs' functions have not yet been determined.

In the present study, we hypothesized that the CBM present in *Cj*Cel9A could provide a significant advantage for immobilizing the multi-domain *Cj*Cel9A cellulase on environmental cellulose (e.g., leaf residues), which is accumulated in sediment and difficult to wash away. Saltwater coastal wetlands, including mangrove forests and tidal flats, are generally considered as carbon sinks that have larger carbon quantity compared to other ecosystems (Pant et al. 2003). The carbon stocks in coastal wetlands were derived from the upstream ecosystems (allochthonous C input) such as forests (Richey et al. 2002, Moomaw et al. 2018), as well as local photosynthesis plant communities such as the reed beds seen in many brackish wetlands in Japan (autochthonous C production) (Sudip et al. 2005, Scholz 2013). In our study site located in Mie Prefecture, central Japan, more than half of the wetland is covered with reed beds, and there is a huge amount of reed leaves in the sediment, which could be a scaffold for secreted cellulase.

To test the hypothesis, we firstly determined the binding function of *Cj*Cel9A-CBM by using a recombinant protein (*Cj*cel9A-CBM^{GFP}) of *Cj*Cel9A-CBM fused with Green Fluorescent Protein (GFP) in its C-terminus as a reporter. In addition, we performed a binding study with varying concentrations of cellulose to evaluate its affinity. Furthermore, crystallinity studies was performed to examine whether Cjcel9A-CBM have different affinity against celluloses varied in the level/type of crystallinity, the result showed that *Cj*cel9A-CBM^{GFP} has superior affinity for highly crystallized cellulose (i.e. Cellulose I, mostly seen in natural sources). Based on the results of these analysis, we finally discuss the function of *Cj*Cel9A-CBM as an anchor of the cellulase secreted from its bivalve producer, and the significance of this function to environmental cellulose decomposition.

Materials and Methods

Materials

Except for specialized reagents indicated in the text, all reagents were purchased from Nacalai Tesque (Kyoto, Japan). Fallen reed (*Phragmites australis*) leaves and *C. japonica* individuals were collected in July 2014 from Tanaka River Estuary, an untouched wetland located in Mie Prefecture, Japan (Kimura & Kimura 1999). All samples were transported to the laboratory in a cooler box with ice packs. Crystalline styles (an unique enzyme storage organ found in bivalves and gastropods) were collected from *C. japonica* individuals and immediately stored at −80°C until use.

Recombinant *Cj*cel9A-CBM^{GFP} expression and purification

The CBM sequence of *Cj*Cel9A (GenBank: BAF38757.1, from Ala^{16} to Pro^{116}) was amplified and fused with a GFP gene at its 5′ end. The recombinant *Cj*cel9A-CBM^{GFP} and GFP (control) were expressed and purified according to our previous report (Liu et al. 2019). Briefly, the *Cj*Cel9A-CBM sequence was amplified using a forward primer 5′-GAG GGA TCC CCA CCA CCA CCA CCA CCA CGC ACC AGT AAC TAT C-3′ with an Immobilized Metal Affinity Chromatography (IMAC, i.e. His_6-tag, used to purify the recombinant protein to minimize the influence of multi-protein interactions that might cause false affinity results and decrease the credibility of further biding studies), and a backward primer of 5′-GAG GGT ACC CCT GGA CCT ACA GAC CT-3′. PCR products were purified and inserted into a pEGFP plasmid (BD Biosciences Clontech) at the N-terminus of GFP with no linker amino acids and transformed into a XL-blue strain of *E. coli*. After pre-culturing in 2 mL of LB medium containing 100 μg mL^{-1} ampicillin at 37°C for 16 h, the transformed *E. coli* was transferred to 200 mL of fresh LB medium and incubated at 37°C for another 4 h before adding isopropyl-β-D-thiogalactoside (IPTG) to a final concentration of 100 μg mL^{-1}. Collected cells were re-suspended in 2 mL of Phosphate-buffered saline (PBS), lysed by sonication on ice and centrifuged at 8,000×g for 20 min. The supernatant was collected as a crude extract of *Cj*cel9A-CBM^{GFP} and purified using a His-trap™ FF column (GE Healthcare) following the manufacturer's protocol and stored at −80°C in the presence of 1 mM NaN_3 before use. As a control, GFP was also expressed and purified. Both recombinant proteins were verified by SDS-PAGE stained with Coomassie Brilliant Blue (CBB).

Antibody purification

The antibody against *Cj*Cel9A was raised in our previous study (Sakamoto et al. 2007). In the present study, we used purified *Cj*cel9A-CBM^{GFP} as ligand to purify the *Cj*Cel9A antibody using a method described in a previous study (Liu et al. 2019), briefly introduced as follows: *Cj*cel9A-CBM^{GFP} recombinant protein purified by IMAC was used as the ligand. Two and a half milligrams of *Cj*cel9A-CBM^{GFP} was desalinized using a Prepacked Disposable PD-10 column (GE Healthcare) and then immobilized on an NHS-activated HP column (GE

Healthcare). Five milliliters of the antiserum were concentrated using a 5,000 Da molecular sieve (Amicon Ultra-15 5,000 MWCO, Millipore) and then introduced to the NHS column and purified following the manufacturer's protocols.

Fluorescence microscopy

To investigate the affinity of *Cj*cel9A-CBM^{GFP} for α-cellulose (Sigma-Aldrich), xylan (a component of plant cell-wall polysaccharides called hemicelluloses, Sigma-Aldrich, from beechwood), and reed leaves collected from Tanaka River Estuary, Mie Prefecture, 40 mL of artificial seawater (REI-SEA Marine, main components contain NaCl, KCl, $CaCl_2$, $MgCl_2$, and Na_2HPO_4. No EDTA and dry seawater powder contained, Iwaki Co. Ltd, same below) and 1 mL of 9 μM *Cj*cel9A-CBM^{GFP} were mixed with 1 mg of each candidate substrate. After shaking at 4°C for 1 h, the substrate was collected and washed with 40 mL of 1 M NaCl three times before fluorescence microscopy. As controls, substrate mixed with GFP or IMAC elution buffer was also observed.

Isotherms of *Cj*cel9A-CBM^{GFP}

One mg of α-cellulose was mixed with *Cj*cel9A-CBM^{GFP} at 10 different final concentrations (6, 3, 1.5, 0.75, 0.57, 0.38, 0.28, 0.19, 0.14 and 0.09 μM, measured by the Bradford method (Bradford 1976), n=5) in PBS (pH=7.4). The α-cellulose was then collected and washed with 1 mL of 1 M NaCl 5 times. After samples were re-suspended in 100 μL of artificial seawater, they were transferred to a flat-bottom 96-well fluorescence plate and the intensity of fluorescence was measured using an image analyzer (FLA-9000, FUJIFILM). The concentration of bound *Cj*cel9A-CBM^{GFP} was calculated by reference to a standard curve of the fluorescence intensity of pure *Cj*cel9A-CBM^{GFP}. A Scatchard plot was applied to calculate the maximum binding capacities (B_{max}), dissociation constant (K_d) and corresponding partitioning coefficients (K_r).

Immuno-scanning electron microscopy

For immuno-scanning electron microscopy (immuno-SEM), the sample was prepared in essentially the same way as described in the above section concerning fluorescence microscopy. The primary anti-*Cj*Cel9A antibody was diluted 1 : 1000, and the secondary antibody (Immune Gold Conjugate EM Goat Anti-rabbit IgG: 15 nm, BBInternational) was diluted 1 : 500. Before samples were analyzed using a scanning electron microscope (TM3000, Hitachi), they were immobilized by adding 1 mL of reagent containing 2% glutaraldehyde and 4% paraformaldehyde and incubated at 4°C for 1 day, and then dried at room temperature for 1 day.

Pulldown assay of *Cj*cel9A-CBM^{GFP}

According to the results of immuno-SEM, the binding of *Cj*Cel9A-CBM^{GFP} to α-cellulose was uneven, but we did not know what kind of feature of α-cellulose could affect the binding behavior. We then decided to investigate if *Cj*Cel9A-CBM showed different affinities to cellulose from different sources. Endogenous *Cj*Cel9A (including CBM domain) was used in this experiment to avoid possible influence of the GFP reporter.

Endogenous *Cj*Cel9A cellulase was collected from approximately 10 crystalline styles and homogenized in 100 μL of PBS. After centrifugation at 8,000×g for 5 min, the protein concentration in the supernatant was measured by the Bradford method (Bradford 1976). One milliliter of PBS, 1 mg of cellulose substrate (α-cellulose, filter paper or reed leaves) and 0.25 mg of crystalline style extract were mixed and incubated at 4°C for 1 h. After the incubation, the cellulose was washed with artificial seawater 5 times and mixed with 20 μL of sample buffer (Laemmli buffer) before separation by electrophoresis on a 7.5% acrylamide gel in the presence of 2-mercaptoethanol, and then transferred to a polyvinylidene difluoride (PVDF, GE Healthcare) membrane. The primary anti-*Cj*Cel9A antibody was diluted 1 : 1,000, and the secondary anti-rabbit IgG (H&L) HRP-linked antibody (Cell Signaling Technology) was diluted 1 : 10,000. High performance autoradiography film (Amersham® Hyperfilm®, GE Healthcare) was used for imaging.

Influence of cellulose crystallinity on *Cj*Cel9A-CBM^{GFP}'s binding

To determine the crystal structure of cellulose, 0.5 g of α-cellulose and filter paper were subjected to X-ray diffraction measurement by the reflection mode using a Rigaku Ultima IV diffractometer with nickel-filtered Cu Kα radiation at 40 kV and 40 mA. To investigate the influence of the crystallinity on the binding strength of *Cj*Cel9A-CBM^{GFP}, filter paper treated with NaOH was also measured as described above. In this case, the filter paper was treated with 17.4% (w/v) NaOH for 1 or 4 hours and washed with 40 mL of distilled water. The binding of *Cj*Cel9A-CBM^{GFP} to NaOH-treated filter paper was then conducted using a similar method to that described above. Briefly, 1 mL of 9 μM *Cj*Cel9A-CBM^{GFP} was mixed with 1 mg of filter paper that had been subjected to each treatment. After shaking at 4°C for 1 h, the substrate was collected and washed with 40 mL 1 M NaCl three times before the fluorescence intensity was measured. Because the filter paper shrunk due to the NaOH treatment, the fluorescence intensities were expressed per unit area of the filter paper.

Statistical analyses

Statistical analyses were carried out using IBM SPSS (ver. 22) and RStudio (ver. 1.2.1335). Bivariate correlation analysis (Pearson correlation coefficients in SPSS, 2-tailed) was used to examine the regression function in the Scatchard plot. One-sample t-test (SPSS) was applied to the results of the relative fluorescence between

α-cellulose and filter paper to compare their affinity for *Cj*Cel9A-CBM^{GFP}. For the comparison of the *Cj*Cel9A-CBM bound on different groups of NaOH-treated filter papers, Levene's Test was used before one-way ANOVA was applied, and then Tukey's HSD post hoc analysis was used (RStudio).

Results

Affinity of *Cj*Cel9A-CBM^{GFP} for α-cellulose and filter paper

To evaluate the affinity of the recombinant *Cj*Cel9A-CBM^{GFP}, pure cellulose (α-cellulose) and reed (*Phragmites australis*) leaves were tested as substrates. As shown in Fig. 1, the CBB-strained bands of both *Cj*Cel9A-CBM^{GFP} and GFP (control) matched each's putative molecular size. No other prominent bands were detected, which means that the purification was sufficient. As shown in Fig. 2, the GFP reporter clearly showed that *Cj*Cel9A-CBM^{GFP} had affinity for both α-cellulose and reed leaves (Fig. 2, top panel). GFP itself showed no affinity for any of the polysaccharides we tested in the present study, indicating that this affinity was not caused by the GFP reporter (Fig. 2 middle panel). Also, none of the substrates showed any auto-fluorescence (Fig. 2, bottom panel). As for xylan, *Cj*Cel9A-CBM^{GFP} showed no affinity. In addition, the affinity for α-cellulose and reed leaves was not influenced by 1 M NaCl used for washing off nonspecifically bound material. Moreover, *Cj*Cel9A-CBM^{GFP} did not bind evenly on reed leaves.

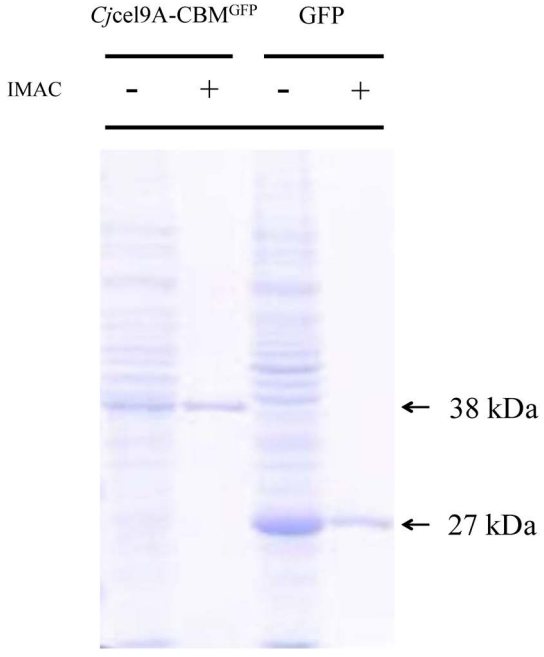

Fig. 1. Purification of recombinant protein. CBB-staining of *Cj*Cel9A-CBM^{GFP}s and GFPs (control) before (−) and after (+) the purification via Immobilized Metal Affinity Chromatography (IMAC). After IMAC, only one prominent band was detected for *Cj*Cel9A-CBM^{GFP} and GFP, and the molecular size of each band matched the putative molecular size according to its amino-acid sequence.

Binding isotherms of *Cj*Cel9A-CBM^{GFP}

We evaluated the binding strength of *Cj*Cel9A-CBM^{GFP} with varying concentrations of α-cellulose. The initial isotherm curve is shown in Fig. 3. Scatchard plot analysis was applied to calculate the dissociation constant ($K_D = 0.352$) and the maximum binding capacity ($B_{max} = 7.156$). The corresponding partitioning coefficient (K_r) was calculated as well by the ratio of B_{max} to K_D ($K_r = B_{max}/K_D = 20.33$).

Binding characteristics of *Cj*Cel9A-CBM^{GFP} on specific region of cellulose

To obtain more detail about how *Cj*Cel9A-CBM^{GFP} bound unevenly to α-cellulose fibers as shown in Fig. 2, immuno-SEM was applied (Fig. 4). The results of immuno-SEM clearly showed that the binding of *Cj*Cel9A-CBM^{GFP} was localized on α-cellulose (Fig. 4, top left and right). In the negative GFP control (Fig. 4, bottom) no signal was detected.

Affinity of crystalline style *Cj*Cel9A for various substrates

After washing with artificial seawater, Western blotting detected the presence of endogenous (crystalline style origin) *Cj*Cel9A cellulase on α-cellulose and filter paper, but not on reed leaves (Fig. 5). Two bands of endogenous *Cj*Cel9A cellulase were detected on substrates. The larger one (67 kDa) was considered to be a precursor (Sakamoto & Toyohara 2009), while the one with the size of 60 kDa matched the putative molecular size of *Cj*Cel9A cellulase, which was reported to exist in wetland sediments in our previous study (Liu et al. 2019).

Influence of crystallinity on *Cj*Cel9A-CBM's binding

To investigate if the different affinities are caused by different crystallinity of different cellulose sources, X-ray crystallography was applied. The results showed that cellulose and filter paper have different crystallography patterns (Fig. 6, a, b). Filter paper had the signature of the Cellulose I crystalline structure (Hidaka et al. 2010), which is more often seen in highly crystallized cellulose. α-cellulose, on the other hand, had no distinguishable signal pattern, which means it was amorphous cellulose. The relative fluorescence intensity of *Cj*Cel9A-CBM^{GFP} on filter paper was almost 10-fold stronger than that on α-cellulose (Fig. 6, c, d). After treatment with NaOH, the crystallography pattern of filter paper became more similar to that of α-cellulose, and its affinity for *Cj*Cel9A-CBM^{GFP} decreased about 8-fold after the treatment of NaOH, while no statistical significance were found between the 2 treatment groups of 1 hour and 4 hours (Fig. 7).

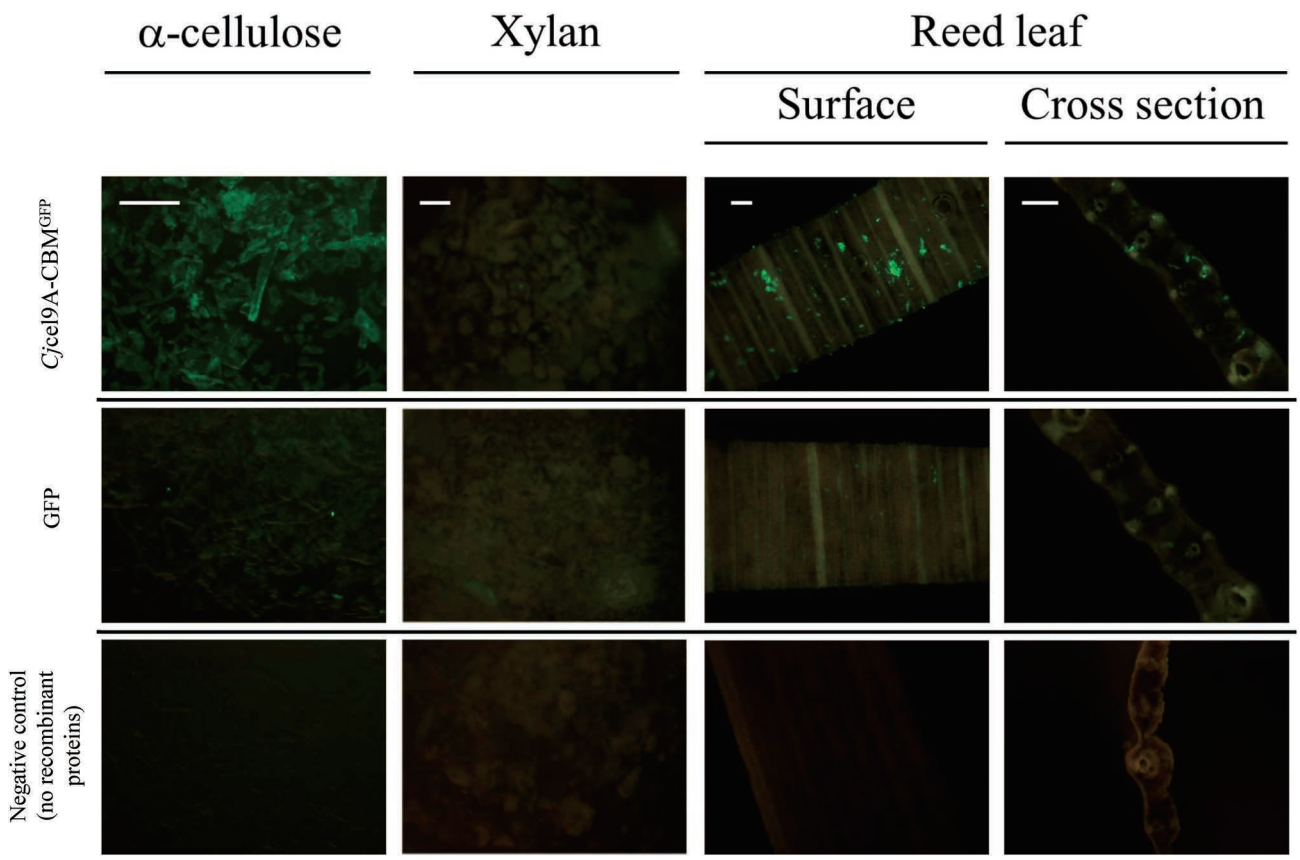

Fig. 2. Affinity of *Cj*Cel9A-CBM^{GFP} for *α*-cellulose, xylan and reed leaves. The binding of *Cj*Cel9A-CBM^{GFP} to *α*-cellulose, xylan (from beechwood) and reed leaf (*Phragmites australis*, both surface and cross section) are shown in columns. Upper panel, fluorescence of *Cj*cel9A-CBM^{GFP} was observed on *α*-cellulose and reed leaves, but not xylan. Middle panel, no fluorescence was observed on any substrate when *Cj*cel9A-CBM^{GFP} was replaced with GFP. Bottom panel, no auto-fluorescence was observed on any substrate (negative controls). Scale bars, 200 μm, shared in the same column.

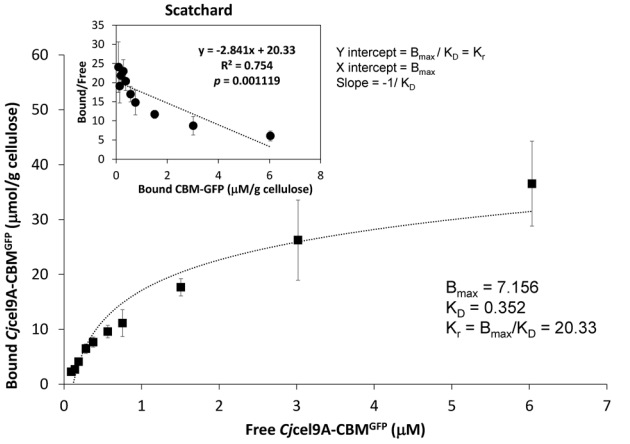

Fig. 3. Isotherms and Scatchard plot of *Cj*cel9A-CBM^{GFP} against *α*-cellulose. The initial isotherm curve is shown as filled black squares. Free *Cj*cel9A-CBM^{GFP}, the concentration of *Cj*cel9A-CBM^{GFP} that was initially mixed with *α*-cellulose. Bound *Cj*cel9A-CBM^{GFP}, *Cj*cel9A-CBM^{GFP} that bound to *α*-cellulose after washing. Scatchard plot is shown in upper left of the isotherm curve. According to the regression function (R^2=0.754, p=0.001119, n=5 for each plot, value=mean±SEM), B_{max}, K_D, and K_r were calculated and are shown at bottom right.

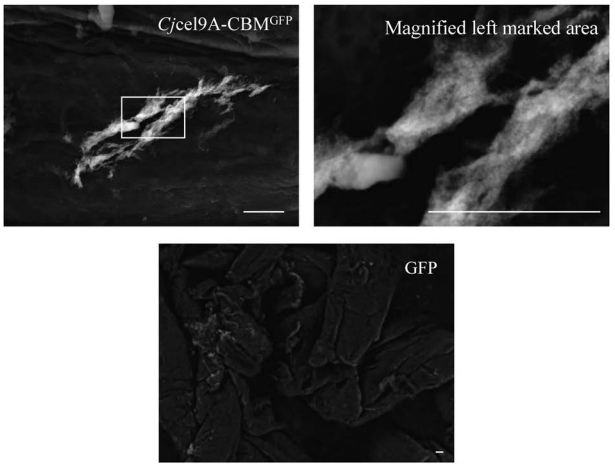

Fig. 4. Immuno-scanning electron microscopy of *Cj*cel9A-CBM^{GFP} bound to *α*-cellulose. Upper left, white regions are the binding sites of *Cj*cel9A-CBM^{GFP} on *α*-cellulose. Upper right, magnified image of the boxed region in the upper left panel. Bottom, negative control in which *Cj*cel9A-CBM^{GFP} was replaced with GFP. Scale bars, 100 μm.

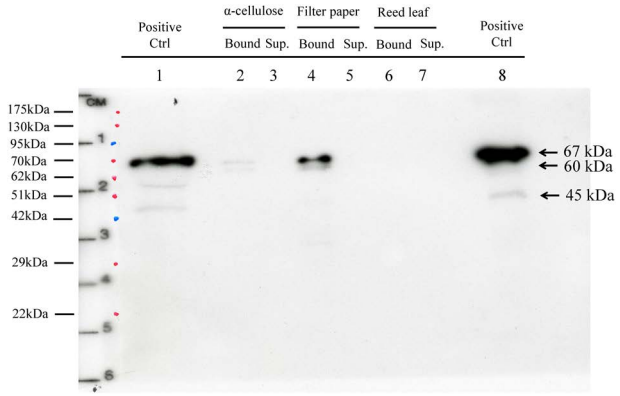

Fig. 5. Affinity of crystalline style *Cj*Cel9A for various cellulose substrates. Bound, endogenous *Cj*Cel9A bound to and eluted from each type of cellulose. Sup., supernatant (washing buffer) fraction obtained by washing off non-specifically bound endogenous *Cj*Cel9A. Two types of endogenous *Cj*Cel9A signals (67 kDa and 60 kDa) were detected. The signal of 60 kDa was the *Cj*Cel9A cellulase, while the signal of 67 kDa was considered to be a precursor of *Cj*Cel9A.

Discussion

The CBM of *Cj*Cel9A was shown here to be capable of binding to α-cellulose and filter paper, which are both pure celluloses. To our knowledge, this is the first study to confirm the function of an aquatic invertebrate CBM. We also showed that *Cj*Cel9A-CBM^{GFP} binds unevenly on reed leaves collected from wetlands (Fig. 2). If the substrate that *Cj*Cel9A-CBM^{GFP} binds on reed leaves is cellulose, the uneven binding might occur because 1) most of the cellulose in reed leaves had already been consumed when the leaves were collected, or 2) the cellulose was not yet fully exposed for some yet unknown reason(s) (plant wax covered the leaves, for example). According to the CAZY database, *Cj*Cel9A-CBM was categorized as a Family 2 CBM based on its nucleotide/amino acid sequence (CAZY Database). The placement in this category suggests its potential ability to bind xylan and chitin. We therefore investigated *Cj*Cel9A-CBM^{GFP}'s affinity for xylan (β-D-1,4-xylopyranose, from beechwood) because it is another type of carbohydrate

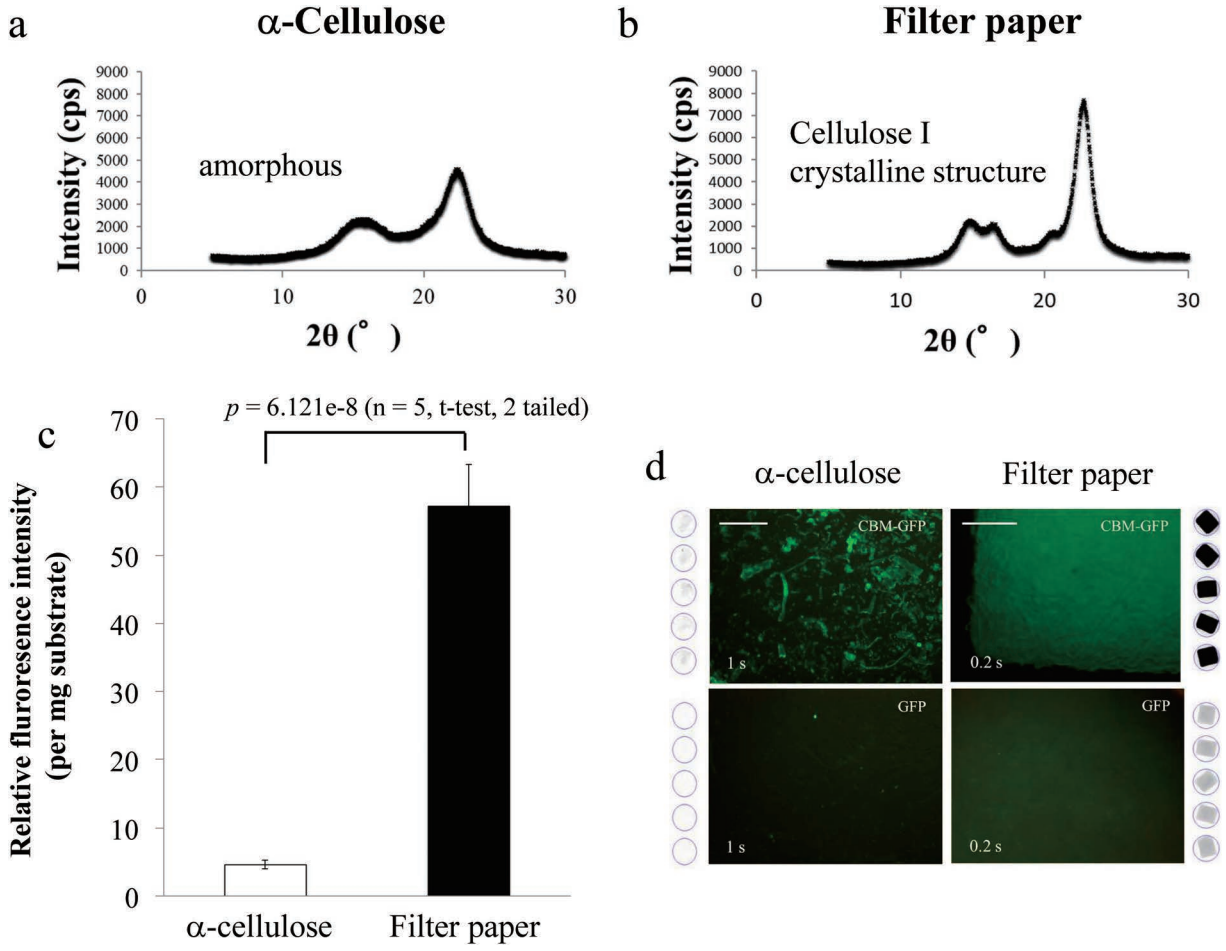

Fig. 6. Relationship between affinity and crystalline structure. a,b. X-ray crystallography of α-cellulose and filter paper, respectively. c. The affinity of *Cj*cel9A-CBM^{GFP} for α-cellulose and filter paper, shown as the relative fluorescence intensity of GFP (n=5, value=mean±SEM). d. Fluorescence microscopy of *Cj*cel9A-CBM^{GFP} bound to α-cellulose (upper left), and filter paper (upper right). Negative controls are shown in the same column (bottom panel). Scale bars, 200 μm, shared in the same column. Alongside each image, the fluorescence intensity was shown as the quantified relative darkness in the fluorescence scan image of each sample (n=5).

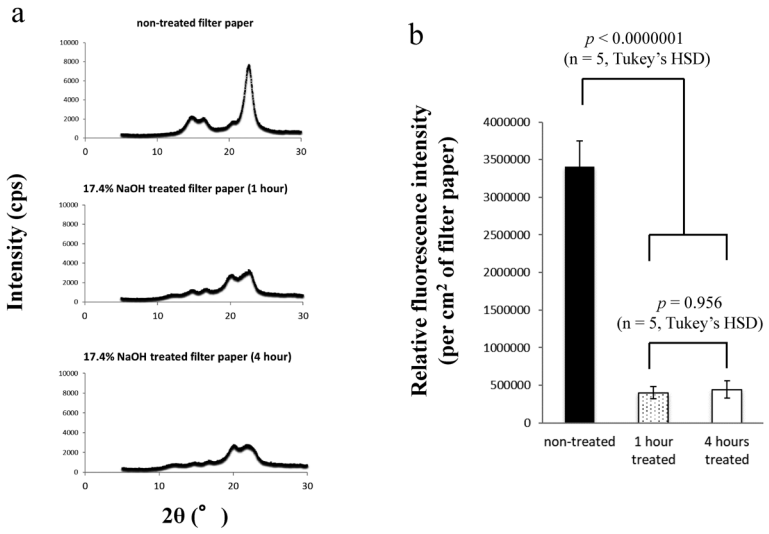

Fig. 7. Influence of cellulose crystallinity to *Cj*cel9A-CBMs' affinity. a. X-ray crystallography of filter paper treated with 17.4% (w/v) NaOH. Upper, non-treated filter paper. Middle, filter paper treated with NaOH for 1 hour. Bottom, filter paper treated with NaOH for 4 hours. b. Relative fluorescence intensity of *Cj*cel9A-CBM^{GFP} bound on filter paper before and after NaOH treatment (n=5, value=mean±SEM).

in the plant cell wall, but the result was negative (Fig. 2). There are multiple types of xylan in different plant species (Amos & Mohnen 2019) and some of them might have affinity for *Cj*Cel9A-CBM^{GFP}; therefore, the true substrate that *Cj*Cel9A-CBM^{GFP} binds on reed leaves remains to be investigated. Wetland sediments contain abundant cellulose, so although the actual binding substrate of *Cj*Cel9A-CBM^{GFP} in reed leaves remains unclear, the ability of *Cj*Cel9A-CBM^{GFP} to bind to both reed leaves and cellulose would enable the *Cj*Cel9A cellulase to be capable of immobilizing itself in wetland sediments. This capability could be one of the reason that secreted *Cj*Cel9A cellulase was detected in wetland sediment (Liu et al. 2019).

As for the level of the binding activity, isotherms and Scatchard plot analysis showed here that *Cj*cel9A-CBM^{GFP} has a Kr value of 20.33 to *α*-cellulose, which is quite high compared to the value obtained in a previous study using chimera CBM modules that originated from the filamentous fungi *Trichoderma reesei* cellulase (Arola & Linder 2016). *Cj*Cel9A-CBM has the potential to replace the CBMs of bacteria and fungi that are now generally used in genetic engineering studies for making high-efficiency chimera cellulases. However, high affinity might not be essential to the efficiency of the decomposition activity. A previous study showed that in some cases, the presence of a CBM could be an obstruction to catalytic efficiency toward high concentrations of lignocellulose substrates (Costaouec et al. 2013). Thus, future studies to examine the compatibility of *Cj*Cel9A-CBM with different catalytic domains and its ability to increase catalytic activities will be required. Notably, in the present study, the relative fluorescence intensity was measured after *Cj*Cel9A-CBM^{GFP}-bound substrate (*α*-cellulose or reed leaves) was washed with 1 M NaCl, of which the ion concentration is approximately 3-fold higher than the ion concentration of natural seawater. This high-salt tolerance feature of *Cj*Cel9A-CBM could be an adaption to its producers' habitats, brackish water wetlands.

We noted that, if we magnified the image sufficiently, it could be seen that the *Cj*Cel9A-CBM^{GFP} did not actually bind to *α*-cellulose ubiquitously (Fig. 2). We confirmed this finding by using immuno-SEM, which showed that *Cj*Cel9A-CBM^{GFP} was localized on *α*-cellulose fibers (Fig. 4). At first, we were confused by this finding, because unlike reed leaves, *α*-cellulose is artificial and pure, which means there would be no problems of "substrate already consumed" or "substrate not exposed" described in the above-noted case of leaf substrates. We also thought that this might have been because of the interference of the GFP reporter or protein-folding alterations caused by separating CBM from its adjacent catalytic domain. However, by investigating the crystalline style *Cj*Cel9A cellulase collected from *C. japonica* individuals, we found that there was an obvious difference between the affinity for *α*-cellulose and filter paper (Fig. 5). The reason that endogenous *Cj*cel9A wasn't detected on reed leaf is considered to be the low concentration of *Cj*cel9A cellulase in crystalline style, compared to the Cjcel9A-CBM^{GFP} recombinant protein used in fluorescent microscopy (Fig. 2). What's important here is that the difference of binding between *α*-cellulose and filter paper could be due to their internal features, such as the level of crystallinity, because *α*-cellulose and filter paper are both pure celluloses produced by different industrial manufacturing procedures. The results of X-ray crystallography showed that the filter paper forms a Cellulose I crystalline structure, which is mostly seen in nature. *α*-cellulose, however, seems to be amorphous, possibly as a result of chemical treatments during its manufacturing process (Fig. 6). Upon treatment with NaOH, the crystallinity of filter paper decreased and became similar to that of *α*-cellulose, and its affinity to *Cj*Cel9A-CBM^{GFP} also decreased significantly (Fig. 7). Since Cellulose I crys-

talline structures occur naturally, the *Cj*Cel9A-CBM^{GFP} will have an inherent advantage for binding to natural cellulose, such as that in plant residues. The reason that *Cj*cel9A-CBM prefers Cellulose I might ascribe to the primary (amino acid sequence), secondary (3 dimensional structure of local protein segment), tertiary (3 dimensional structure of the whole mono-protein), or quaternary (arrangement of multiple folded protein subunits) structure of the CBM. To date, there are few studies about aquatic invertebrates' CBM, and the studies focused on microorganism's CBM already indicated that the function of each CBM are difficult to be judged just by their primary structure. Thus, further experiments using purified or recombinant CBMs are required to unravel the relationship between CBMs' molecular structure and their functions.

Based on those findings, we can conclude that *Cj*Cel9A-CBM could work efficiently on wetland sediments. It is impossible to infer the significance of this CBM to wetlands just from its functions, but it is also true that a mechanism that could immobilize the secreted *Cj*Cel9A cellulase to the sediment is needed to explain the following two facts that are now widely recognized in the field of wetland environmental studies. The first one is that sediment in many wetlands holds cellulase activities, even in wetlands that are being washed almost every day. At first, these activities were ascribed to microorganisms such as bacteria and fungus and small invertebrates known as meio-benthos. However, our previous study showed that even when all meio-benthos were excluded with sieves and microorganisms' growth was suppressed with antibiotics, the cellulase activity still remained (Liu et al. 2012). This means that, in addition to secreted cellulase, other cellulases, which we called "environmental enzymes", which are localized independent of their producers, also exist in wetland sediments. The second fact is the involvement of large invertebrates, known as macro-benthos. As noted in the introduction, endogenous cellulase has been discovered in macro-benthos recently, but the connection between these enzymes and wetland sediment had not been revealed until our recent study showed that *C. japonica* individuals secrete their cellulase (*Cj*Cel9A) into the sediment (Liu et al. 2019). We also confirmed the existence of *Cj*Cel9A cellulase in the total extract of proteins of the sediment at Tanaka River Estuary by using immunological methods (Liu et al. 2019). These findings suggested a novel cellulose decomposition system in wetland sediment, which involves not only organisms, but also enzymes that might be secreted by physiological processes, excreted in feces, or released from the dead bodies of their producers. This decomposition system (which we called an "environmental bioreactor system" in Liu et al. 2019) could partially explain how cellulase activ-

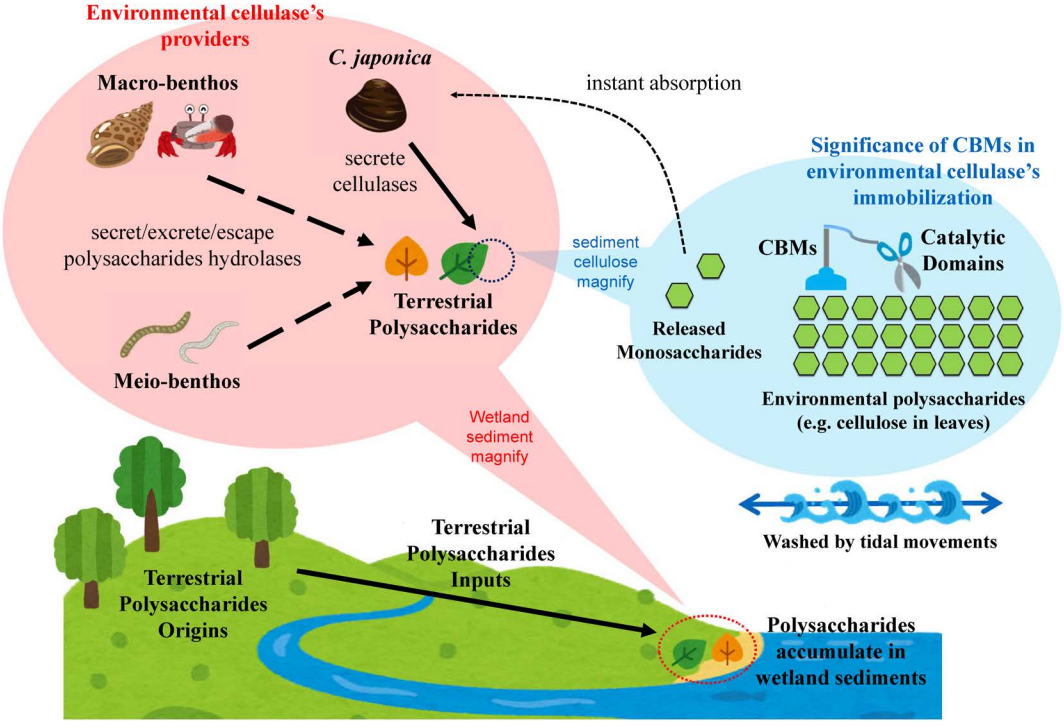

Fig. 8. Possible roles of *Cj*Cel9A-CBM and other CBMs in wetland sediments. Endogenous *Cj*Cel9A cellulase of *C. japonica* was reported to exist in the wetland sediment in our previous study (continuous line arrow in red frame) (Liu et al. 2019). Along with the CBM in this polysaccharide hydrolase, other CBMs produced by various aquatic invertebrates are also thought to exist and be immobilized in wetland sediments (dotted line arrows in red frame). Wetland sediments are constantly washed by seawater. The CBMs present in glycoside hydrolases (which were secreted/excreted/escaped from their providers) immobilize their adjacent catalytic domains by using environmental polysaccharides as scaffolds (blue frame). The wetland sediment thus becomes an "environmental bioreactor" that could constantly decompose terrestrial polysaccharides.

ity could exist constantly in wetland sediments.

However, all these observations lacked an explanation of exactly how these enzymes escape being washed away, since they are easily dissolved in water. As shown in Fig. 8, the present study focused on the CBM domain of *Cj*Cel9A, and suggested that it could be the anchor that immobilizes environmental enzymes such as the *Cj*Cel9A cellulase secreted by *C. japonica*, on leaves, which are much larger than the enzyme itself, and can more easily stay in the sediment, and thus avoid being washed away.

In summary, *Cj*Cel9A-CBM was proven to have high affinity for natural cellulose (Cellulose I). Also, *Cj*Cel9A-CBM is highly functional in high ion concentration environmental conditions, such as the conditions in brackish wetland sediments. These properties support the notion that the possession of CBMs by aquatic invertebrates might be one of the reasons that cellulase activities are constantly and widely detected in many wetland sediments. Moreover, this "CBM anchor" might be one of the most essential feature that empowers the wetlands to be a key player in the decomposition of terrestrial plant cell-wall polysaccharides.

Acknowledgements

This work was supported by Grants-in-Aid for Scientific Research from the Ministry of Education, Culture, Sports, Science, and Technology of Japan (Nos. 21380131, 25292113, 12J04439, 25660167, 22405030, and 17H03851).

References

Amos RA, Mohnen D (2019) Critical review of plant cell wall matrix polysaccharide glycosyltransferase activities verified by heterologous protein expression. Front Plant Sci 10: 1–27.

Arola S, Linder MB (2016) Binding of cellulose binding modules reveal differences between cellulose substrates. Sci Rep 6: 35358.

Boraston AB, Bolam DN, Gilbert HJ, Davies GJ (2004) Carbohydrate-binding modules: fine-tuning polysaccharide recognition. Biochem J 382: 769–781.

Bradford MM (1976) A rapid and sensitive method for the quantitation of microgram quantities of protein utilizing the principle of protein-dye binding. Anal Biochem 72: 248–254.

Carbohydrate-Active enZYmes Database. Available at: http://www.cazy.org/. (accessed on 2 Dec 2019).

Costaouec TL, Pakarinen A, Varnai A, Puranen T, Viikari L (2013) The role of carbonhydrate binding module (CBM) at high substrate consistency: compare of *Trichoderma reesei* and *Thermoascus aurantiacus* Cel7A (CBHI) and Cel5A (EGII). Bioresour Technol 143: 196–203.

Hidaka H, Kim UJ, Wada M (2010) Synchrotron X-ray fiber diffraction study on the thermal expansion behavior of cellulose crystals in tension wood of Japanese poplar in the low-temperature region. Holzforschung 64: 167–171.

Kimura S, Kimura T (1999) The gastropod fauna of the marshes of the reed (*Phragmites australis* (Cav.)) in the estuaries in Mikawa Bay and Ise Bay, Japan. Jpn J Benthology 54: 44–56.

Li Y, Yin Q, Ding M, Zhao F (2009) Purification, characterization and molecular cloning of a novel endo-beta-1,4-glucanase AC-EG65 from the mollusc *Ampullaria crossean*. Comp Biochem Physiol B, Biochem Mol Biol 153: 149–156.

Liu. W, Toyohara H (2012) Sediment-complex-binding cellulose breakdown in wetlands of rivers. Fish Sci 78: 661–665.

Liu W, Tanimura A, Nagara Y. Watanabe T, Maegawa S, Toyohara H (2019) Wetland environmental bioreactor system contributes to the decomposition of cellulose. Ecol Evol 9: 8013–8024.

Moomaw WR, Chmura GL, Davies GT, Finlayson CM, Middleton BA, Natali SM, Perry JE, Roulet N, Sutton-Grier AE (2018) Wetlands in a changing climate: science, policy and management. Wetlands 38: 183–205.

National Center for Biotechnology Information. Genbank No.: ABO26609.1, BAD44734.1, *Haliotis discus discus*. National Center for Biotechnology Information. Available at: https://www.ncbi.nlm.nih.gov/ (accessed on 1 Dec 2019).

Pant HK, Rechcigl JE, Adjei MB (2003) Carbon sequestration in wetlands: concept and estimation. JFAE 1: 308–313.

Richey JE, Melack JM, Aufdenkampe AK, Ballester VM, Hess LL (2002) Outgassing from Amazonian rivers and wetlands as a large tropical source of atmospheric CO_2. Nature 416: 617–620.

Sakamoto K, Touhata K, Yamashita M, Kasai A, Toyohara H (2007) Cellulose digestion by common Japanese freshwater clam *Corbicula japonica*. Fish Sci 73: 675–683.

Sakamoto K, Toyohara H (2009) Putative endogenous xylanase from brackish-water clam *Corbicula japonica*. Comp. Biochem. Physiol. B, Biochem. Mol Biol 154: 85–92.

Scholz M (2013) Wetland systems storm water management control. In: Carbon Storage and Fluxes Within Wetland Systems. Springer, London, pp. 127–140.

Shoseyov O, Shani Z, Levy I (2006) Carbohydrate binding modules: biochemical properties and novel applications. MMBR 70: 283–295.

Sudip M, Reiner W, Paul LGV (2005) An appraisal of global wetland area and its organic carbon stock. Curr Sci 88: 25–35.

Suzuki K, Ojima T, Nishita K (2003) Purification and cDNA cloning of a cellulase from abalone *Haliotis discus hannai*. Eur. J Biochem 270: 771–778.

Tanimura A, Liu W, Yamada K, Kishida T, Toyohara H (2013). Animal cellulases with a focus on aquatic invertebrates. Fish Sci 79: 1–13.

Tilbeurgh V.H, Tomme P, Claeyssens M, Bhikhabhai R, Pettersson G (1986) Limited proteolysis of the cellobiohydrolase I from *Trichoderma reesei*. FEBS Lett 204: 223–227.

Tomme P, Tilbeurgh VH, Pettersson G, Damme VJ, Vandekerckhove J, Knowles J, Teeri T, Claeyssens M (1988) Studies of the cellulolytic system of *Trichoderma reesei* QM 9414: Analysis of domain function in two cellobiohydrolases by limited proteolysis. Eur J Biochem 170: 575–581.

Watanabe H, Tokuda G (2001) Animal cellulases. Cell Mol Life Sci 58: 1167–1178.

Zhang G, Fang X, Guo X, Li L, Luo R, et al. (2012) The oyster genome reveals stress adaptation and complexity of shell formation. Nature 490: 49–54.